EPSC Abstracts
Vol. 13, EPSC-DPS2019-676-1, 2019
EPSC-DPS Joint Meeting 2019

EPSC
EPSC-DPS Joint Meeting 2019
15–20 September 2019 | Geneva, Switzerland

Venus Nighttime Photochemical Model: Nightglow of O_2, NO, OH and Abundances of O_3 and ClO

Vladimir A. Krasnopolsky
Moscow Institute of Physics and Technology (PhysTech), Moscow, Russia (vlad.krasn@verizon.net)

Abstract

The observed morphology of the nightglow emissions and abundances of O_3 and ClO provide important constraints to the photochemical structure of the nighttime atmosphere and fluxes of atomic species from the day side. The proposed model reproduces these phenomena.

1. Introduction

Detections and first studies of Venus' nightglow were made four decades ago using the Venera 9-10 [8,6] and Pioneer Venus [15] orbiters and ground-based high-resolution spectroscopy [2,13]. Later, long-term observations by Venus Express in 2005-2014 provided the most detailed studies of the O_2 nightglow at 1.27 μm [11] and in the visible range [4] and the NO UV nightglow [5,16]. The NO band at 1.224 μm [3] and the OH rovibrational bands [10,14] were discovered on Venus. Nighttime ozone layers near 95 km [9] were detected using the SPICAV stellar occultations from Venus Express. Recently ClO [12] was detected on the Venus night side using ground-based high-resolution spectroscopy in the submillimeter range.

All these phenomena refer to the altitude range of 85-120 km in the nighttime atmosphere. Lifetimes of atoms, radicals, and some molecules are smaller than the duration of Venus' night (≈2 Earths days) at these altitudes. Therefore the global-mean models are inapplicable for comparison with observations of short-living species on the night side. Here we update our previous nighttime photochemical model [7] using the recent detection of ClO.

2. Model

The nighttime chemistry at 80-130 km is induced by transport of atomic species from the day side, where the density at 150 km exceeds that of the night side at this altitude by a factor of ≈30. The model involves 86 reactions of 29 species. Downward fluxes of O, N, H, and Cl at 130 km are the model parameters to fit the observed mean intensities of the O_2, NO, OH nightglow and abundances of O_3 and ClO. The chosen fluxes are $\Phi_O = 3\times10^{12}$, $\Phi_N = 1.2\times10^9$, $\Phi_H = 9\times10^9$, and $\Phi_{Cl} = 4\times10^9$, all in cm^{-2} s^{-1}. The model chemistry converts the flux of O at 130 km completely to flux of O_2 at 80 km, the flux of N to flux of N_2, the fluxes of H and Cl return a flux of HCl at 80 km, and the excess of H over Cl returns almost equal fluxes of H_2 and H_2O formed by the reactions of HCl with H and OH, respectively. Flux of CO $\Phi_{CO} = 2\times10^{12}$ cm^{-2} s^{-1} is included to simulate the nighttime CO bulge and returned unchanged at 80 km. The calculated mean nighttime composition of the atmosphere is shown in Fig. 1.

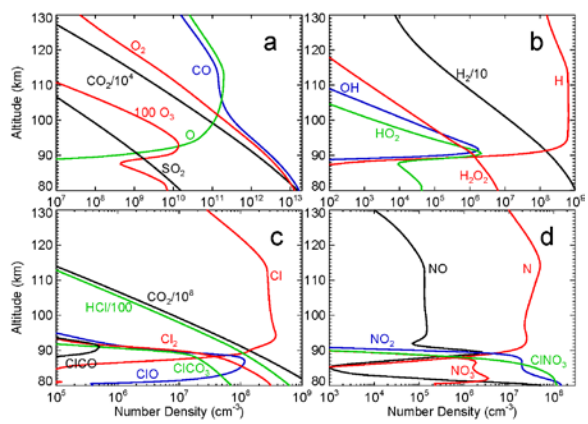

Fig. 1. Chemical composition of the mean nighttime atmosphere at 80-130 km: (*a*) CO_2 products and SO_2, (*b*) hydrogen species, (*c*) chlorine species, and (*d*) nitrogen species.

The measured ClO [12] is either 2.6 ± 0.6 ppb in a 10 km layer at 90 km or 2.3 ± 0.5 ppb at 85-100 km (Fig. 2). The model profile of the ClO mole fraction peaks at 88 km with f_{ClO} = 4.3 ppb and full width at half maximum FWHM = 3.7 km. Averaging of the mole fraction within 10 km gives 1.7 ppb at 87.5 km, while a ratio of the averaged ClO and total density is 2.3 ppb at 90.5 km (Fig. 2). The same for the layer at 85-100 km is 2.2 ppb. Therefore the model agrees with the observed ClO.

The calculated ozone (Fig. 1a) peaks at 93 km with $[O_3] = 1.4\times10^8$ cm^{-3} and FWHM = 6.3 km. Its peak limb column abundance is 7.8×10^{15} cm^{-2}, in accord with the SPICAV occultations [9].

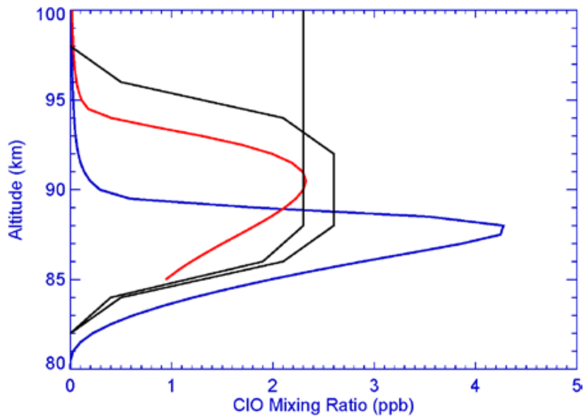

Fig.2. ClO mixing ratio in the model (blue) and that in a ten-km layer (red) are compared with those adopted in [12] to fit their observations

Calculated vertical profiles of the nightglow of O_2, NO, and OH are shown in Fig. 3. Here we assume that the OH nightglow is excited by H + O_3 → OH(v) + O_2 only. The observed mean nightside intensities of the OH bands (1-0), (2-1), (3-2), and (4-3) are 2.74, 2.40, 0.57, and 0.44 kR, respectively [14,7]. The adopted yields of v" in quenching of OH (v') by CO_2 are those of the collisional cascade model v" = v' – 1 with corrections to fit the observed line distribution.

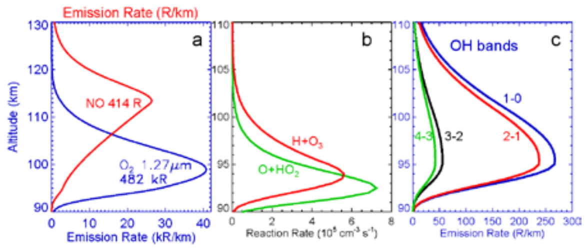

Fig. 3. Calculated vertical profiles of the O_2, NO, and OH nightglow and two reactions that may form OH(v)

The fluxes of O, N, H, and Cl are properly chosen to fit the observed mean nightglow intensities and the abundances of O_3 and ClO. However, the model does not have parameters to fit the observed altitudes of the nightglow and species layers. Peaks of volume emission rate are typically ≈2 km above those observed on the limb. The excellent agreement of the model with the observations confirms adequacy of the model.

3. Variations of the nighttime composition and nightglow

The fluxes of O, N, H, and Cl vary on the night side and result in variations of the nightglow and abundances of O_3 and ClO. The model is a convenient tool to study these variations. While the predicted variations of the nightglow and O_3 are moderate, those of ClO may exceed two orders of magnitude. Major reactions that control ClO are

$Cl + O_3 \rightarrow ClO + O_2$; $k_1 = 2.3\times10^{-11}\, e^{-200/T}$ cm^3 s^{-1}

$ClO + O \rightarrow Cl + O_2$; $k_2 = 2.8\times10^{-11}\, e^{85/T}$ cm^3 s^{-1}.

If transport is neglected, then

$$[ClO] \approx 0.8\, e^{-285/T}\, [Cl][O_3]/[O].$$

All species involved are highly variable near 90 km (Fig. 1).

Variations of the O_2, NO, OH nightglow and abundances of O_3 and ClO may be approximated by analytic relationships that make it possible to convert the fluxes into nightglow intensities, O_3 and ClO abundances and vice versa. Modeling of dynamic and composition of the Venus upper atmosphere, including fluxes from the day side to the night side and their variations, are among the problems under consideration by the Venus Thermosphere GCM, and some results on this subject are presented in [1].

References

[1] Brecht A.S. et al. JGR 116, E08004, 2011
[2] Connes P. et al. Astrophys. J. 233, L29-L32, 1979
[3] Garcia Munoz A. et al. Proc. Nat. Acad. Sci. 106,985-988, 2009
[4] Garcia Munoz A. et al. JGR 114, E12002, 2009
[5] Gerard J.C. et al. JGR 113, E00B03, 2008
[6] Krasnopolsky V.A. In "Venus" (Hunten D.M. et al., ed.), Univ. Arizona Press, USA, pp. 459-483, 1983
[7] Krasnopolsky V.A. Planet Space Sci. 85, 78-88, 2013
[8] Krasnopolsky V.A. et al. Cosmic Res. 14, 789-795, 1976
[9] Montmessin F. et al. Icarus 216, 82-85, 2011
[10] Piccioni G. et al. Astron. Astrophys. 483, L29-L33, 2008
[11] Piccioni G. et al. JGR 114, E00B38, 2009
[12] Sandor B.J. and Clancy R.T. Icarus 313, 15-24, 2018
[13] Slanger T.G. et al. Science 291, 463-465, 2001
[14] Soret L. et al. Planet. Space Sci. 73, 387-396, 2012
[15] Stewart A.I.F. et al. JGR 85, 7861-7870, 1980
[16] Stiepen A. et al. Icarus 226, 428-436, 2013